JOURNAL OF CATALYSIS 90, 119–126 (1984)

CO Chemisorption on Ru/SiO_2: The Influence of Coadsorbates[1]

HSIU-WEI CHEN, ZHENG ZHONG, AND J. M. WHITE

Department of Chemistry, University of Texas, Austin, Texas 78712

Received September 1, 1983; revised June 19, 1984

The adsorption of CO at room temperature on SiO_2-supported Ru was studied in a static system by Fourier transform–infrared. Three bands were observed in the infrared spectra at ca. 2030, 2080, and 2140 cm^{-1}. Isotopically mixed CO adsorption suggests that the bands at 2030 and 2140 cm^{-1} are the result of $Ru(CO)_n$, $n \geqq 1$. The relative band intensities varied with pretreatment (oxidation, reduction, and evacuation). When a second element like O or Cl was coadsorbed with CO on the Ru surface, the band at 2080 cm^{-1} was the strongest. The band at 2030 cm^{-1} dominated the spectra when CO was adsorbed alone on a reduced surface. It was broad and comprised of multiple bands assigned to $Ru(CO)_n$, $n \geqq 1$. The bands at 2080 and 2140 cm^{-1} are assigned to $Ru(CO)X_m$ and $Ru(CO)_nX_m$, where X represents H_2O (or OH), O, or Cl. Isotope labeling experiments show that the CO(a) corresponding to the band at 2030 cm^{-1} was the easiest to exchange with gas-phase molecules, suggesting it is the least tightly held.

INTRODUCTION

Ruthenium is well-known as a hydrogenation catalyst, especially for CO methanation; (*1*) however, the interaction mechanism of H_2 and CO with the supported Ru has not been well characterized. Whether the coadsorption of the two reactants and/or other species leads to variation in chemical bond strengths and, through that, to changes in the reactivity of adsorbed species is an interesting question. We chose infrared spectroscopy as a method for studying how coadsorbed species alter the properties of adsorbed carbon monoxide, CO(a).

Adsorption of CO on supported Ru has been intensely studied by ir (*2–4*), but little work has been reported regarding coadsorption (*5*). In general, the results for CO(a) are consistent above 2000 cm^{-1} where bands are observed at 2030, 2080, and 2140 cm^{-1}. Several different models have been proposed to interpret these spectra, including a multiple coordination model (*6, 7*), an oxidation state model (*8–10*), and a particle size model (*11*). As the results reported here demonstrate, none of these is entirely satisfactory.

We have reinvestigated, using ir, the CO/Ru system with and without coadsorbed species; particularly, CO with H, O, and Cl. Our results indicate the importance of interactions between these coadsorbates.

EXPERIMENTAL

A 4 wt% Ru/silica catalyst was prepared by impregnating Cab-O-Sil, grade HS-5 (Cabot Corp.) with an aqueous solution of $RuCl_3 \cdot 3H_2O$ (Aldrich). The resulting gel was dried in air at 100°C for 16 hr. Carbon monoxide was purified through a 5 Å molecular sieve trap maintained at 77 K. ^{13}CO was used as received. H_2 was purified through a Pd catalyst and a 5 Å molecular sieve trap at 77 K. The ir cell was a standard design which permitted evacuation and heating of the sample under static conditions. Calcium fluoride windows were used. Spectra were taken using a Nicolet 7199 FT–IR spectrometer (300 scans) and were recorded at room temperature in absorbance form with a resolution of 2 cm^{-1}. All spectra reported here have been corrected by subtraction for adsorption of the gas

[1] Supported in part by the Office of Naval Research.

0021-9517/84 $3.00

phase, blank catalyst disk, and CaF_2 windows.

To make a 1-in.-diameter disk, roughly 100 mg of the catalyst was spread uniformly on paraffin paper (to prevent metal contamination) and pressed at 5000 psi. The exact weight was chosen to given reasonable ir spectra. The resulting disk was heated under vacuum at 325°C for 1 hr. Prior to an adsorption experiment, the catalyst disk was typically oxidized with 1 atm O_2 for 16 hr at temperature T_1, evacuated at 325°C for 1 hr, reduced with 1 atm H_2 for 16 hr at temperature T_2, and evacuated at a particular temperature, T_3, and time interval, t, of interest. The following symbol is used to represent the oxidation, reduction, and evacuation temperature sequence: (T_1, T_2, T_3, t). For example (325-325-425-1 hr) means oxidation at 325°C for 16 hr, reduction at 325°C for 16 hr, and evacuation at 425°C for 1 hr.

The average crystallite size of the supported Ru was determined from X-ray line broadening using the (101) line of Ru and from hydrogen adsorption. Good agreement between electron microscopy and hydrogen chemisorption has been demonstrated for similar Ru systems (*12*).

RESULTS

Before taking up the individual experiments, we make the following comments. In the spectra described below, we give the *measured* peak positions for each case. These fall into, and will be discussed in terms of, three bands at ca. 2030, 2080, and 2140 cm^{-1}. In order to get better resolution of the three CO bands on Ru/SiO_2, we added the oxidation step (typically at 325°C for 16 hr) before the reduction step. Without this additional step, the particle size was estimated as 60 Å for a (no-325-425-1 hr) sample, and the CO bands at 2080 and 2030 cm^{-1} were not as well resolved as with the oxidation step (325-325-425-t), where the average particle size was 110–140 Å. The CO adsorption bands were less intense for the latter because of the larger particle size, and they were less strongly overlapped.

Figure 1 shows the spectra for several different pretreatment steps followed by exposure to 15 Torr of CO. Figure 1a is for a sample evacuated at 325°C for 1 hr, with no oxidation or reduction steps so the metal was still oxidized and chloride was present. The major band is at 2088 cm^{-1}. Spectrum 1b is for a (no-325-425-1 hr) sample that was not oxidized, but was reduced to remove chloride and reduce the metal. The particle size is around 60 Å, and the most intense peak is at 2039 cm^{-1}. Spectrum 1c is the sample from 1b followed by degassing at 325°C for 1 hr, oxidation at 325°C for 10 hr,

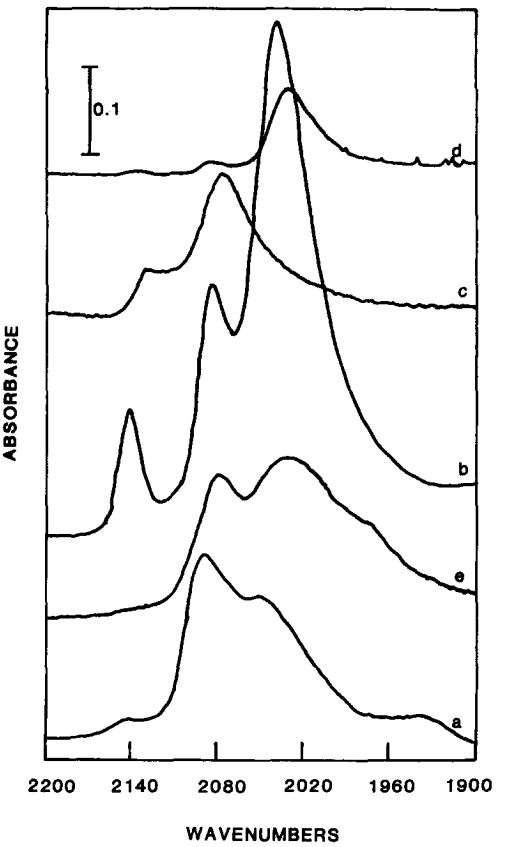

FIG. 1. CO adsorption (15 Torr) on (a) (no-no-325-1 hr) sample, (b) (no-325-425-1 hr), (c) 10 hr at 325°C in O_2 after (b) followed by evacuation at 425°C for 1 hr, (d) 16 hr at 325°C in H_2 after (c) followed by evacuation at 425°C for 1 hr, and (e) 15 Torr $^{13}CO/^{12}CO$ (1 : 1) on (no-no-325-1 hr) sample.

and evacuation at 425°C, 1 hr. Here, the metal is oxidized and the band at ca. 2030 cm^{-1} disappears, while the other two peaks are shifted to slightly lower frequencies. Spectrum 1d is the sample from 1c followed by degassing at 325°C for 1 hr, reduced in H_2 at 325°C overnight, and degassed at 425°C for 1 hr. It has the same features as the (no-325-325-1 hr) sample of Fig. 1b, but with much weaker bands. The lower adsorption intensity was due, at least in part, to the bigger Ru particle size (110 Å). Spectrum 1e is the (no-no-325-1 hr) sample of Fig. 1a except the adsorbed gas was a $^{13}CO/^{12}CO$ equimolar mixture. No band splitting was observed, but a new band was resolved at 1978 cm^{-1}.

Figure 2 shows other spectra for the coadsorption of an equimolar mixture of ^{13}CO and ^{12}CO on a (325-325-425-1) sample. In order to get higher infrared absorption intensities, the disk was made from 200 mg Ru/SiO_2. Four bands, 2134, 2084, 2020, and 1981 cm^{-1}, were observed. The band at 2134 cm^{-1} is due to ^{12}CO; it is split into two peaks at 2134 and 2125 cm^{-1} (see a′, b′, and c′) which are interpreted (see below) in terms of multiple coordination on one site, the higher frequency arising from multiple ^{12}CO coordination and the lower arising from mixed ^{12}CO and ^{13}CO. The band at 2084 cm^{-1} is from two different CO adsorption sites; one is the original ^{12}CO(a), the other from ^{13}CO(a) which corresponds to the ^{12}CO band at 2134 cm^{-1}. The shoulder on the high-frequency side of the 2084-cm^{-1} band appears because of the slightly different position of these two bands. The band at 2020 cm^{-1} also comes from ^{12}CO and ^{13}CO adsorbed at different Ru sites with the major intensity from ^{12}CO. Finally, the band at 1981 cm^{-1} is from ^{13}CO. Its absorbance is smaller than the corresponding band (2020 cm^{-1}) for ^{12}CO. This is unexpected for an equimolar mixture of ^{12}CO and ^{13}CO, but has also been observed by Cant and Bell (*13*). A model involving multiply coordinated CO is proposed to explain this result and will be discussed below.

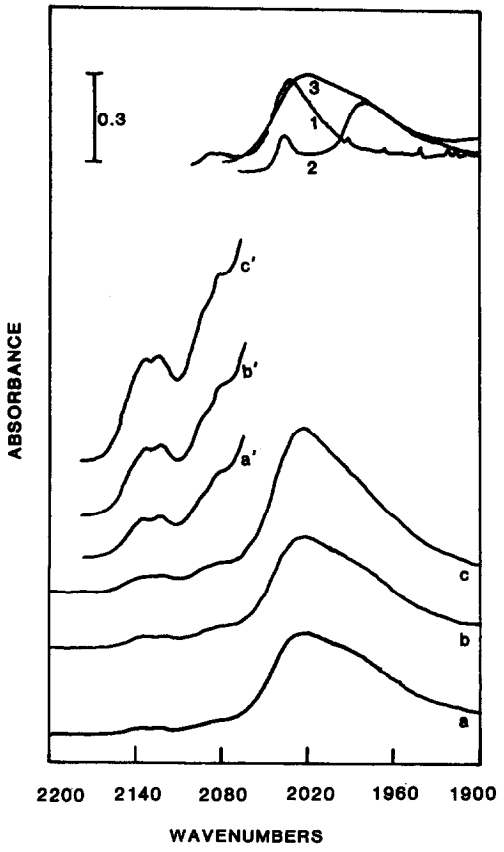

FIG. 2. Adsorption of $^{12}CO/^{13}CO$ (1 : 1) on Ru/SiO_2 (325-325-425-1 hr). (a) 15 Torr $^{12}CO/^{13}CO$ for 4 min, (b) 70 min, (c) coadsorption of $^{12}CO/^{13}CO/H_2$ for 30 min with P_{CO} = 15 Torr and P_{H_2} = 22 Torr. The primed spectra are six-fold expansions of the unprimed spectra. The inset shows separate spectra for 15 Torr of (1) ^{12}CO, (2) ^{13}CO, and (3) 1 : 1 mixture.

Figure 3 shows the isotope exchange between preadsorbed ^{13}CO and gas-phase ^{12}CO. Three bands are observed at 1981, 2037, and 2085 cm^{-1} after dosing 15 Torr ^{13}CO for 10 min or 24 hr (Figs. 3a and b). These correspond to the bands at 2036, 2085, and 2137 cm^{-1} observed for ^{12}CO (Fig. 1d). The intensity of the 1981-cm^{-1} band decreased about 50% (Fig. 3c) after evacuation of the ^{13}CO for 10 min at room temperature, while the intensity of the other two bands was unchanged. The shape of the 1981-cm^{-1} band is indicative of more than one state. Upon subsequent adsorption of 15 Torr ^{12}CO at room temperature

(Figs. 3d, e, and f), the ^{13}CO band at 1981 cm^{-1} exchanged rapidly with gas-phase ^{12}CO, and after a 1-hr exposure it disappeared completely (Fig. 3e). During the same period, the intensity of the 2085-cm^{-1} band did not change, and no ^{12}CO band appeared around 2135 cm^{-1}. Slowly (~1 day) the spectrum became like that for the adsorption of ^{12}CO at 15 Torr and room temperature.

Figure 4 shows the stability of the three adsorbed CO states under vacuum after exposure of a (325-325-425-2) sample to CO. After a 10-min evacuation, the area of the bands at 2136, 2085, and 2035 cm^{-1} (Fig. 4b) decreased to 87.7, 86.3, and 62.3% of the area of the corresponding bands in Fig. 4a.

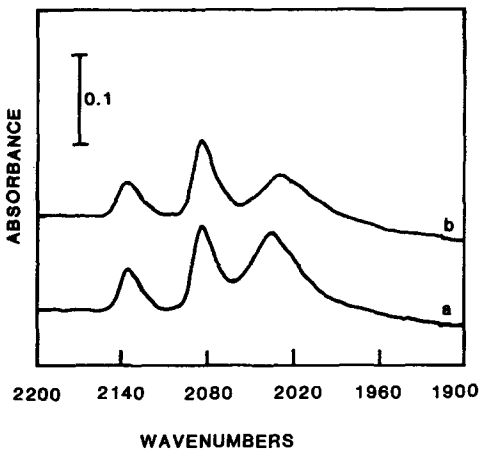

FIG. 4. Properties of a (325-325-425-2 hr) sample. (a) following adsorption of 15 Torr CO for 1 day and (b) after evacuation at room temperature for 10 min.

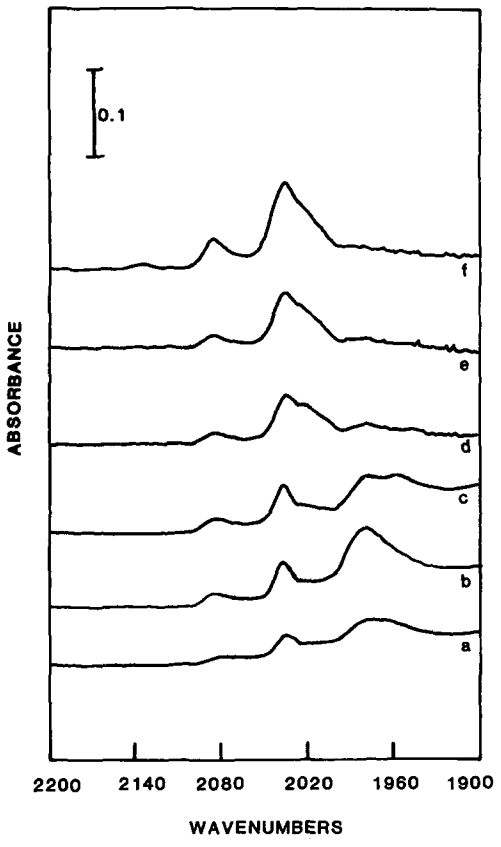

FIG. 3. Exchange of ^{12}CO with presorbed ^{13}CO on Ru/SiO_2 (325-325-425-1 hr). (a) ^{13}CO (15 Torr) for 10 min, (b) 1 day, (c) under vacuum at room temperature for 10 min, (d) postadsorption of 15 Torr ^{12}CO for 8 min, (e) 1 hr, and (f) 1 day.

This is consistent with the exchange results above and suggests that the species giving rise to the 2035-cm^{-1} band is relatively weakly bound.

Having established the exchangeability and stability of adsorbed CO, experiments were conducted to determine the effect of hydrogen and oxygen on CO adsorption on Ru/SiO_2. When CO was adsorbed on a sample predosed with oxygen at 300 K, the band at 2078 cm^{-1} was the strongest (Fig. 5a). After evacuation of CO and dosing 160 Torr of H_2 for 30 min, the CO peaks shifted from 2130, 2078, and 2020 cm^{-1} (Fig. 5a) to 2143, 2080, and 2034 cm^{-1} (Fig. 5c) and showed a characteristic intensity distribution of CO adsorption on a reduced Ru surface (see Fig. 1d). A very different result was obtained when sample 5c was treated with O_2 and CO just as in Fig. 5a and was followed by exposure to 160 Torr of CO/H_2 (1 : 10) gas mixture. Figure 5d shows the recovery to the conditions of Fig. 5a, and Fig. 5e shows the result of exposure to the CO and H_2. The intensity of the bands at 2028 and 2136 cm^{-1} increased and gradually shifted to the region 2050 and 2140 cm^{-1}, while the intensity of the band at 2083 cm^{-1} decreased and shifted up to 2086 cm^{-1}.

In the former case, we suppose that hydrogen reacts with oxygen to form water

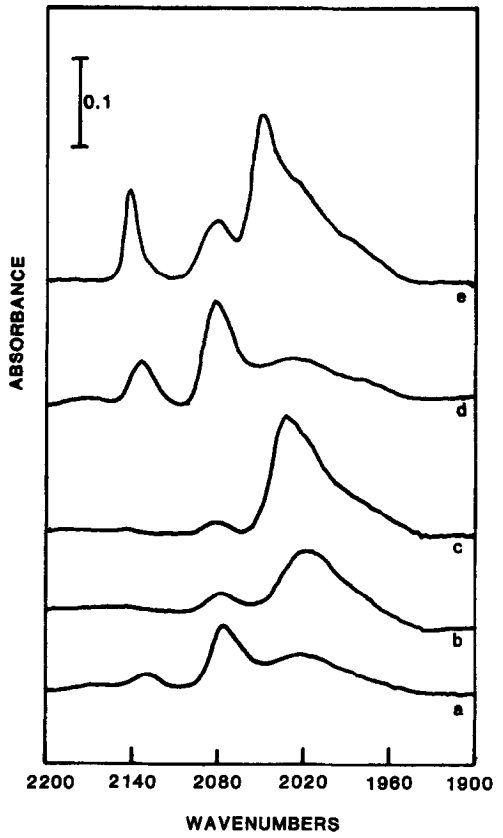

FIG. 5. Hydrogen, oxygen, and carbon monoxide interactions on Ru/SiO_2 (325-325-425-1 hr) at room temperature. (a) Adsorption of 10 Torr O_2 at room temperature for 2 min, evacuation for 1 min, then adsorption of 16 Torr CO at room temperature for 10 min and evacuation for 1 min, (b) dose H_2 160 Torr at room temperature for 5 min, (c) 30 min, (d) evacuation for 1 min and repetition of procedure (a). (e) Following adsorption of CO/H_2(1/10) 160 Torr at room temperature for 30 min.

which is either desorbed immediately or is displaced when CO is added. In the latter case, there is some reaction to form water, but the reaction does not go to completion because strongly bound CO blocks H_2 chemisorption.

DISCUSSION

(*A*) *Band Assignment*

Our spectra are consistent with previous reports, but the models presented cannot fully describe our results. Kobayashi and Shirasaki report two bands in the region 1900–2100 cm^{-1} and predict the existence of $Ru(CO)_3$ based on the CO/Ru uptake ratios (*6*) and EPR spectra (*14*). These authors did not report detailed frequencies, and we suspect that their experimental conditions precluded detection of the three bands we report here. The effect of the Ru particle size (Al_2O_3 support) on the spectrum of adsorbed CO has been discussed by Dalla Betta (*11*). On a sample with an average particle size greater than 90 Å, only one band at ca. 2030 cm^{-1} was seen, while three CO bands were observed when the average particle size was less than or equal to 60 Å. Multiple adsorption of CO on coordinatively unsaturated Ru sites was proposed based on measured CO/H uptake ratios (*11*). In contrast, we find three bands on our (325-325-425-1 hr) sample which had an average particle size greater than 100 Å as measured by X-ray line broadening and hydrogen chemisorption methods. It is clear that average particle size alone is an insufficient explanation; there may also be an effect of the support. For example, the particle size distribution and the preferred Ru surface structure may depend on the support.

Brown and Gonzalez (*8*) suggested that the ca. 2030-cm^{-1} band is due to the linear and dominant CO species on fully reduced Ru, that the ca. 2080-cm^{-1} band is linear CO on oxygen-perturbed Ru and that the ca. 2140-cm^{-1} band is CO on strongly oxidized Ru, e.g., RuO_n. When a strongly reduced Ru/SiO_2 sample is exposed to O_2 and then CO at room temperature (Figs. 5a and d), we do reproduce the results of Brown and Gonzalez (*8*) in that the ca. 2080-cm^{-1} band dominates the spectrum. However, when CO is adsorbed on heavily oxidized Ru/SiO_2 (Fig. 1c), the dominant band is still at 2080 cm^{-1}. According to the oxidation-state model, there should be a shift to the 2140-cm^{-1} region with this treatment. Moreover, under some conditions the intensity of the band at 2140 cm^{-1} actually increases with time in a reducing atmosphere (Fig. 5e). We conclude that the oxi-

dation-state model cannot fully explain the observed behavior.

With these literature results in mind, we proceed to assign the bands observed in our experiments. The framework of previous descriptions is expanded by adding the concept of frequency shifts due to coadsorption. The band at ca. 2030 cm^{-1} is assigned to CO adsorption on fully reduced Ru sites unperturbed by coadsorbed species for the following reasons. When CO was adsorbed on a clean, heavily reduced Ru surface, only one major band was observed at ca. 2030 cm^{-1} (Fig. 1d). Previous workers also report that the 2030-cm^{-1} band is the strongest for a newly reduced Ru sample (*15*). Adsorption of CO on heavily oxidized Ru/SiO_2 did not show this band (Fig. 1c).

When a second species is coadsorbed with CO on Ru/SiO_2, the CO adsorption spectra are dominated by a band at ca. 2080 cm^{-1}. For example, CO on $RuCl_x/SiO_2$ (Fig. 1a), CO on oxygen dosed Ru/SiO_2 (Fig. 5a), and CO on strongly oxidized Ru/SiO_2 (Fig. 1c). When the second element is removed, the strongest band moves back to the 2030-cm^{-1} region. As one example, when $RuCl_3$ was reduced by H_2 and evacuated, the major band changed from 2089 to 2039 cm^{-1} (Figs. 1a to b). Second, comparing an oxidized with a nonoxidized sample, the dominant band moved from 2078 to 2031 cm^{-1} (Figs. 1c to d). Based on these observations, we propose that the 2080-cm^{-1} band is due to CO adsorption on Ru sites which are strongly interacting with a second species like O, Cl, or OH.

The band at ca. 2140 cm^{-1} always appears with the band at 2080 cm^{-1}. We expect that they arise from similar adsorbed species. Davydov and Bell (*10*), based on correlated band intensities, assigned these two bands to the symmetric vibrations of a pair of CO molecules adsorbed on a common Ru^+ site. In our data, the intensity ratio of the bands 2080 and 2140 cm^{-1} is not constant. For example, this ratio varied from less than 0.1 (Figs. 1a and 5a) to greater than 1 (Fig. 5e). Thus, these bands cannot be fully accounted for on the basis of the symmetric and antisymmetric stretch of the same species. At least two *different* species are required. This is best illustrated by comparing Figs. 5d and e. When a mixture of CO and H_2 is exposed to an oxygen-covered surface, the 2080-cm^{-1} band decreases in intensity, but the 2144-cm^{-1} band increases. Clearly, the intensities are not derived from the same species in this case. We believe that the intensity increase of the band at 2140 cm^{-1} is due to multiple CO coadsorption with either an intermediate or a product of the reaction of H_2 and O(a) to give a local structure of the form $Ru(CO)_nX$; X = H, OH, or H_2O. Generally, CO is more strongly bound than H on Ru so CO could replace some of the H(a) or OH(a) and partially block the reaction between hydrogen and oxygen. In this way the intensity of the band at 2140 and 2030 cm^{-1} would both increase, and some intensity near 2080 cm^{-1} would remain.

Further support for this conclusion comes from the isotope results of Figs. 1 and 2. In Fig. 2, the 2140-cm^{-1} band is clearly split when an isotopic mixture of ^{13}CO and ^{12}CO is adsorbed. The peak and shoulder near 2080 cm^{-1} cannot be accounted for in this way because one must first account for ^{12}CO and ^{13}CO adsorbed on *different* Ru sites, both contributing in this region. Further confirmation comes by comparing Figs. 1a and e. The 2140-cm^{-1} intensity in Fig. 1a is very small; thus, adsorption of ^{13}CO on this site will contribute very little to the 2080-cm^{-1} range of Fig. 1e. If coadsorption of ^{13}CO and ^{12}CO split the 2080-cm^{-1} band, it should be observed in Fig. 1e but is not.

The 2030-cm^{-1} band maximum shifted down upon adsorption of an equimolar isotope mixture, and the distribution of intensity differed from the sum of ^{12}CO and ^{13}CO. (See the insert of Fig. 2; curve (3) is not the sum of (1) and (2).) Careful examination of this band in every spectrum shows it is asymmetric and has a shoulder between 2000 and 2020 cm^{-1}, indicating

that it, too, is comprised of at least two distinct species.

When the surface coverage increases, the bands at 2030 and 2140 cm^{-1} shift to significantly higher frequency, while there is only a small shift of the 2080-cm^{-1} bands, suggesting that the CO–CO interactions (i.e., crowding) are more important for the former than for the latter. The splitting of the band at 2140 cm^{-1} by isotopic coadsorption, the broadening of the asymmetric band at 2030 cm^{-1} and the greater crowding of CO adsorption on sites at 2140 and 2030 cm^{-1} are taken as evidence that multiple coordination of CO is involved. As noted earlier, multiple coordination has been a common theme for CO adsorption on Ru (*6, 7, 11, 14, 16*).

To summarize, we assign the three CO bands as

2030-cm^{-1} region: $Ru(CO)_n$

$n = 1, 2 \ldots$

2080-cm^{-1} region: $Ru(CO)X_m$

2140-cm^{-1} region: $Ru(CO)_nX_m$

$X = H_2O$ (or OH, H), O, Cl . . .

The asymmetric 2030-cm^{-1} band observed in our work may come from two or more small bands which correspond to similar sites with different numbers of CO, but we expect the dominance of $n = 1$. In passing, we note that the observation of resolved symmetric/asymmetric pair bands for various values of n in $Ru(CO)_n$ is not necessarily expected, as can be seen in Table 1 for the $Ru(CO)_n(PF_3)_m$ series. For these molecules, there is only one major CO stretching frequency around the 2040-cm^{-1} region.

TABLE 1

Compound	CO stretching frequency	References
$Ru(CO)(PF_3)_4$	2070s, 2026w	(*10, 17*)
$Ru(CO)_2(PF_3)_3$	2078w, 2038s, 2026w, 2007vw	(*10, 17*)
$Ru(CO)_3(PF_3)_2$	2084vw, 2071mw, 2041s, 2026w, 2008w	(*10, 17*)
$Ru(CO)_4(PF_3)$	2106w, 2087w, 2041s, 2027w, 2008w	(*10, 17*)

Another factor is also noteworthy. The metal surface dipole selection rule indicates that only those vibrational modes with dipoles oscillating perpendicular to the metal surface can strongly absorb radiation (*18, 19*). Assuming a structure for $Ru(CO)_n$ in which the molecular axes of CO is oriented away from the surface normal (say to roughly 45°), the asymmetric stretching mode has only a small dipole component perpendicular to the surface, and its infrared absorption intensity is expected to be weak compared with the intensity of the symmetric stretching band.

(*B*) *Stability*

The isotope exchange experiment (Fig. 3) suggests that the CO adsorption corresponding to the band at ca. 2030 cm^{-1} (for ^{12}CO) is relatively weakly held and thus readily exchanges with gas-phase molecules, while the reverse is true for the bands at ca. 2080 and 2140 cm^{-1}. The same result is found on evacuation of adsorbed ^{12}CO, a result confirming other work (*4*). Because of the small difference between the spectra before and after evacuation on the (325-325-425) series sample (the area of the bands at 2140 and 2080 cm^{-1} in Fig. 4b was about 87.7 and 86.3% of the bands area in Fig. 4a), we cannot determine the relative stability of the CO giving the bands at 2080 and 2140 cm^{-1}. Various band stability reports have appeared. Brown and Gonzalez (*8*) and Davydov and Bell (*10*) suggested that the order of stability is 2140 < 2080 < 2030 cm^{-1}; however, this conclusion can be questioned since it is based on spectra in which the lower frequency bands were poorly resolved and the spectra were recorded in transmittance, making it difficult to quantitatively compare the band intensities.

The bonding of CO to Ru is determined largely by two factors: (1) forward bonding, i.e., electron shift from the 5σ orbital of CO to the metal and (2) back bonding, i.e., electron donation into the $2\pi^*$ orbital of CO from the metal *d* band. Increasing the latter

is expected to give a downward shift to the CO stretching frequency. Under our conditions the electron density on Ru is highest for the fully reduced metal, and we expect the forward bonding between the CO and the metal may be weaker in this case than when an electronegative element is present. Turning to the backbonding, it is possible that the electronegative element withdraws *d*-electron density from the metal and lowers the backbonding contribution. The change of the Ru–CO bond strength involves changes in both.

Thus, if there is a decrease in the backbonding contribution brought about by the presence of a coadsorbate, the CO stretching frequency is expected to increase. If at the same time the forward bonding is increased because of the redistribution of electron density on the Ru, then the Ru–CO bond strength will increase in the presence of the coadsorbed species as we observe here.

CONCLUSIONS

Based on both the literature and the results reported here, we draw the following conclusions:

(1) The presence of a coadsorbate can significantly alter the bonding of CO to Ru. This is reflected in changes of the distribution of ir intensity between the bands at ca. 2030, 2080, and 2140 cm^{-1}.

(2) The band at 2140 cm^{-1} can be populated in a reducing gas-phase environment, showing that its structure does not necessarily involve heavily oxidized Ru atoms.

(3) At least two distinct species are required in any explanation of the 2080- and 2140-cm^{-1} bands.

(4) Coadsorption of ^{12}CO and ^{13}CO provides strong support for a multiply coordinated species contributing to the 2140-cm^{-1} band.

(5) Under some conditions (in this case, the presence of a coadsorbate), CO is adsorbed so that the lowest CO stretching frequency (2030 cm^{-1}) is associated with the most weakly held species.

ACKNOWLEDGMENT

We express our thanks to Professor J. G. Ekerdt for providing the catalyst and participating in valuable discussions.

REFERENCES

1. Dalla Betta, R. A., Piken, A. G., and Shelef, M., *J. Catal.* **35,** 54 (1974).
2. Kavtaradze, N. N., and Sokolova, N. P., *Dokl. Phys. Chem. (Engl. Transl.)* **162,** 420 (1965) (Russian: p. 847).
3. Unland, M. L., *J. Catal.* **31,** 459 (1973).
4. Schwank, J., Parravano, G., and Gruber, H. L., *J. Catal.* **61,** 19 (1980).
5. Miura, H. M., McLaughlin, M. L., and Gonzalez, R. D., *J. Catal.* **79,** 227 (1983).
6. Kobayashi, M., and Shirasaki, T., *J. Catal.* **28,** 289 (1973).
7. Goodwin, J. G. Jr., and Naccache, C., *J. Catal.* **64,** 482 (1980).
8. Brown, M. F., and Gonzalez, R. D., *J. Phys. Chem.* **80,** 1731 (1976).
9. Abhivantanaporn, P., and Gardner, R. A., *J. Catal.* **27,** 56 (1972).
10. Davydov, A. A., and Bell, A. T., *J. Catal.* **49,** 332 (1977).
11. Dalla Betta, R. A., *J. Phys. Chem.* **79,** 2519 (1975).
12. Dalla Betta, R. A., *J. Catal.* **34,** 57 (1974).
13. Cant, N. W., and Bell, A. T., *J. Catal.* **73,** 257 (1982).
14. Kobayashi, M., and Shirasaki, T., *J. Catal.* **32,** 254 (1974).
15. Sheppard, N., and Nguyen, T. T., *Adv. Infrared Raman Spectrosc.* **5,** 67 (1978).
16. Bossi, A., Carnisio, G., Garbassi, F., Giunchi, G., Petrini, G., and Zanderighi, L., *J. Catal.* **65,** 16 (1980).
17. Udovich, C. A., and Clark, R. J., *J. Organomet. Chem.* **36,** 355 (1972).
18. Dignam, M. J., Rao, B., and Roth, J., *J. Chem. Soc. Faraday Soc. Trans. 2* **69,** 804 (1973).
19. Pearce, H. A., and Sheppard, N., *Surf. Sci.* **59,** 205 (1976).